Inorganic Chemistry

Article

pubs.acs.org/IC

Enhanced Guest Affinity and Enantioselectivity through Variation of the Gd^{3+}[15-Metallacrown-5] Side Chain

Joseph T. Grant, Joseph Jankolovits, and Vincent L. Pecoraro*

Department of Chemistry, University of Michigan, Ann Arbor, 930 N. University Ave, Ann Arbor, Michigan 48109, United States

Supporting Information

ABSTRACT: Supramolecular hosts that bind guests reversibly are investigated for potential catalysis and separations applications. Chiral Ln^{3+}[15-Metallacrown-5] metallocavitands bind carboxylate guests in hydrophobic cavities generated by their ligand side chains. A thermodynamic study on Gd^{3+}[15-metallacrown-5] hosts with ligands bearing phenyl side chains containing 0, 1, and 2 methylene spacers (**1**-pgHA, **1**-pheHA, **1**-hpheHA, respectively) is presented to quantitatively assess how guest affinity and chiral selectivity can be enhanced through changes to the ligand side chain. Guest binding affinity was measured with cyclic voltammetry using ferrocene carboxylate as a redox probe. K_a values between ferrocene carboxylate and **1**-pgHA and **1**-pheHA were 4800 ± 400 M^{-1} and 4400 ± 700 M^{-1}, respectively. Significantly stronger binding affinity of 12100 ± 700 M^{-1} was measured with **1**-hpheHA, a result of the longer side-chains more completely encapsulating the guest. A similar trend was observed with benzoate. The side chain also influenced enantioselectivity, as K_S/K_R values of up to 2.2 ± 0.6 were measured. The side chain dependent guest binding supports the development of highly selective Ln^{3+}[15-Metallacrown-5] hosts for use in catalysis and separations through careful ligand design.

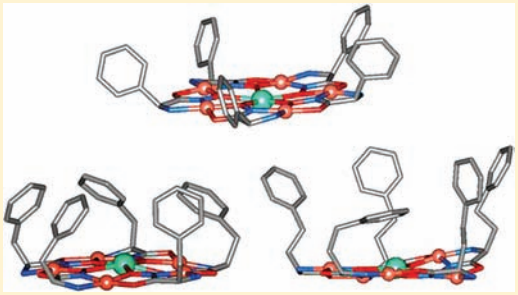

INTRODUCTION

Reversible substrate binding in artificial receptors is a fundamental phenomenon with broad implications.[1] In materials science, guest binding is an emerging method for preparing polymers,[2] gels,[3] and ordered solids.[4,5] Supramolecular catalysts are being developed that use weak, reversible interactions to facilitate transformations of bound guests.[6,7] Selective guest binding to supramolecular hosts is also relevant to separations, sensing, and the resolution of enantiomers.[8−13]

On the basis of the broad implications of reversible guest binding, there is continued interest in supramolecular hosts that selectively bind a chemical substrate. Metallocavitands are a class of supramolecular host characterized by hydrophobic cavities and exposed metal ions.[14] Though significantly less developed than more traditional organic hosts, the metal ions in metallocavitands can contribute to stronger interactions with anionic guests[15−17] and the emergence of catalytic, magnetic, spectroscopic, or electrochemical properties.[18−20] Fabbrizzi and others have used metallocavitands to prepare fluorescent sensors.[21,22] Reports of selective guest transformations in Kersting's dimetallic thiophenolate complexes[23,24] and catalytic reactions in other metallocavitands[25,26] further exemplify the promise of this class of supramolecular host.

One type of metallocavitand with promising anion recognition behavior are chiral Ln^{3+}[15-$Metallacrown_{Cu(II)}$-5] complexes (Figure 1). Metallacrowns (MCs) are a class of metallamacrocycle that serve as inorganic analogues of crown ethers.[27−30] Ln^{3+}[15-$MC_{Cu(II)}$-5] complexes contain a planar metallamacrocycle[31] with a lanthanide central metal surrounded by five Cu^{2+} ring metals. Chirality is introduced in Ln^{3+}[15-$MC_{Cu(II)}$-5] complexes through synthesis with enantiopure hydroxamic acids derived from α-amino acids. The resolved chiral centers on α-amino hydroximate ligands disrupt the mirror plane of symmetry through the MC plane, generating inherent chirality[32] because of the rotational sense of the MC ring. Hydrophobic side-chains on the ligands, such as S-phenylalanine hydroxamic acid (pheHA), drape over one face of the MC, forming a hydrophobic cavity and leaving the other face unencumbered and hydrophilic.[33] These MCs are stable in aqueous solutions at neutral pH and do not racemize.[34−36]

The high metal density and chirality of Ln^{3+}[15-$MC_{Cu(II)}$-5] metallocavitands have spurred interest in their molecular recognition chemistry. In the solid state, single molecule magnets,[37] mesostructures,[38] and dipolar solids that display second-harmonic generation[39] have been realized from Ln^{3+}[15-$MC_{Cu(II),\ pheHA}$-5] complexes. Crystal structures of Ln^{3+}[15-$MC_{Cu(II)}$-5] metallocavitands most commonly reveal dimeric compartments. These compartments assemble via π-stacking interactions between phenyl side chains and selectively encapsulate dicarboxylate guests.[40−42]

In aqueous solutions, monomeric Ln^{3+}[15-$MC_{Cu(II),\ pheHA}$-5] metallocavitands selectively bind carboxylate guests through both coordination to the metal ions and interactions with the phenyl side chains, with binding constants on the order of 10^2–

Received: January 16, 2012
Published: May 2, 2012

   dx.doi.org/10.1021/ic300110g | Inorg. Chem. 2012, 51, 8034−8041

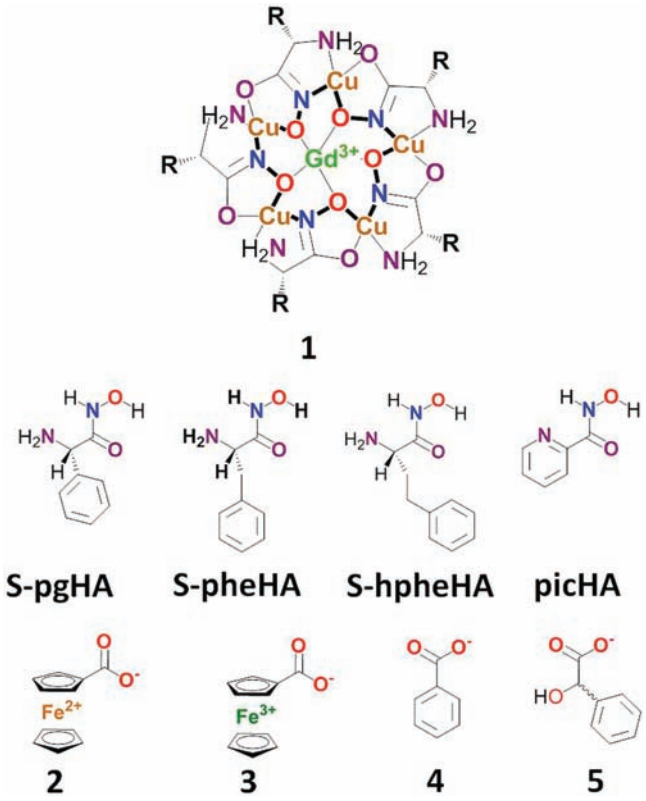

Figure 1. Chemdraw illustrations of the Gd^{3+}[15-$MC_{Cu(II)}$-5] scaffold (**1**), MC ligands, and carboxylate guests. Guests: **2** = ferrocene carboxylate, **3** = ferrocenium carboxylate, **4** = benzoate, **5** = mandelate.

10^4 M^{-1} in aqueous conditions.[36] It has recently been shown that Gd^{3+}[15-$MC_{Cu(II),\ pheHA}$-5]Cl_3 (**1**-pheHA) exhibits modest enantioselectivity for phenylalanine and mandelate (**5**, Figure 1, K_S/K_R = 1.6 and 1.22, respectively).[43] Isothermal titration calorimetry[44] and cyclic voltammetry[45] revealed that guest binding strength increases with more Lewis-acidic lanthanides, suggesting that carboxylates bind to the central metal. Tegoni et al. reported that Eu^{3+}[15-$MC_{Cu(II),\ S\text{-}pheHA}$-5] has a significantly greater affinity for benzoate (**4**, Figure 1) than acetate (K_a = 389 ± 9 M^{-1} and 98 ± 3 M^{-1}, respectively).[46] The reverse trend is expected based on guest basicity, demonstrating that the hydrophobic cavity plays a significant role in guest binding. Guest binding in the hydrophobic cavity is also commonly observed in crystal structures of host−guest complexes.

One potential advantage of Ln^{3+}[15-$MC_{Cu(II)}$-5] metallocavitands is their modular synthesis, which could allow for straightforward tuning of their molecular recognition behavior through variation of the side-chain on the α-amino hydroxamic acid ligand. To date, the effect of different side chains on guest selectivity has only been investigated with solid state dimeric compartments. Ln^{3+}[15-$MC_{Cu(II),\ S\text{-}tyrHA}$-5] compartments form short ∼7.5 Å compartments because of coordination of the phenol to a Cu^{2+} ring metal on the associated MC. These short compartments selectively encapsulate nitrate over chloride.[47] A recent crystallographic study[48] of Ln^{3+}[15-$MC_{Cu(II)}$-5] complexes with S-phenylglycineHA (S-pgHA), S-pheHA, and S-homopheHA (hpheHA) ligands (Figure 1) reveal compartments ranging from 9.7−15.2 Å in height that encapsulate bridging carboxylates. The longer side-chains lead to taller compartments that encapsulate longer guests. Furthermore, the length and flexibility of the side-chain was shown to influence the number of encapsulated guests in the compartments.

Herein a systematic thermodynamic study is reported that examines how structural variation of the Gd^{3+}[15-$MC_{Cu(II)}$-5] phenyl side chain influences guest affinity and selectivity. The primary goal of this study is to quantitatively demonstrate for the first time that guest affinity and chiral selectivity can be enhanced by altering the Ln^{3+}[15-$MC_{Cu(II)}$-5] side chain. These results contribute to the development of highly selective Ln^{3+}[15-$MC_{Cu(II)}$-5] metallocavitands for use in chiral separations and catalysis through optimization of structural substituents on the host. In a broader sense, this systematic study quantitatively demonstrates the extent that peripheral organic substituents can influence guest recognition at a metal center in metallocavitands. In this study, the binding affinity of carboxylates **2**, **3**, and **4** were measured to examine the effect of different side chains. The impact of side chain substitution on enantioselectivity was assessed with S- and R-**5**. Binding affinities are measured with cyclic voltammetry[49] and our recently reported voltammetric competitive binding assay[45] using ferrocene carboxylate (**2**) as a redox probe. S-pgHA, S-pheHA, and S-homopheHA side chains were investigated to assess the effects of increased cavity size and flexibility on guest affinity. Picoline hydroxamic acid (picHA), which generates a planar MC, was also examined to consider guest binding in the absence of a cavity. This thermodynamic study reveals enhanced guest binding strength and enantioselectivity with Gd^{3+}[15-$MC_{Cu(II)}$-5] hosts through side chain substitutions.

EXPERIMENTAL SECTION

All chemicals were used as received unless otherwise described. Ferrocene was recrystallized from pentane. Brockman I activated basic alumina (Aldrich) was utilized for MC purification. S-pheHA, S-pgHA, S-hpheHA,[48] **1**-pheHA(NO_3),[42] picHA[50] and sodium ferrocene carboxylate[45] were prepared as previously described. Sodium salts of mandelate were prepared by neutralization with an equivalent of sodium bicarbonate and stored in a vacuum desiccator over phosphorus pentoxide. Sodium hydroxide solutions were standardized by colorimetric titration against dry potassium hydrogen phthalate with a phenolphthalein indicator. ESI-MS was performed on a Micromass LCT-TOF Electrospray Ionization mass spectrometer with a sample cone voltage of 50 V. ESI-MS solutions were injected via syringe pump in the indicated solvents.

Gd(III)[15-$MC_{Cu(II),\ N,\ S\text{-}pheHA}$-5]$Cl_3$. S-pheHA (0.901 g, 5.00 mmol) was stirred in 35 mL of methanol and deprotonated with 2 equiv of 1 M aqueous sodium hydroxide (10.0 mmol). Stirring continued until all of ligand had dissolved. $GdCl_3$ (0.383 g, 1.03 mmol) and $CuCl_2$ (0.879 g, 5.16 mmol) were sequentially added, and the solution was stirred overnight. The pH of the solution was adjusted to ∼7. After 20 min of stirring, the solution was filtered. Five millliters of 0.5 M aqueous sodium chloride was added to the filtrate, and purple crystals of the product formed by slow evaporation of the solvent. The crystals were isolated by filtration, rinsed with 5 mL of cold water, and air-dried. Yield = 1.4781 g, 86%. CHN Analysis for [($C_{45}H_{50}N_{10}O_{10}Cu_5Gd$)-$Cl_3(H_2O)_{14}$], found (calc'd): C = 31.36 (31.36), H = 4.50 (4.60), N = 8.15 (8.12). ESI-MS (methanol) gave m/z = 690.9^{2+} (691.0^{2+} calc'd for $[GdCu_5(pheHA)_5(OH)]^{2+}$).

Gd(III)[15-$MC_{Cu(II),\ N,\ S\text{-}hpheHA}$-5]$Cl_3$. S-hpheHA (1.00 g, 5.16 mmol) was stirred 30 mL of methanol and deprotonated with 2 equiv of 1 M aqueous sodium hydroxide (10.32 mmol). Stirring continued until all of the ligand had dissolved. $GdCl_3$ (0.383 g, 1.03 mmol) and $CuCl_2$ (0.879 g, 5.16 mmol) were sequentially added, and the solution was stirred overnight. The solution was then gravity filtered and passed through a 5 cm tall activated basic alumina shortpad in a 60 mL fine glass fritted funnel. The short pad was further rinsed with ∼75 mL of a 3:1 methanol/acetonitrile solution (v/v). The recovered solution was

dx.doi.org/10.1021/ic300110g | Inorg. Chem. 2012, 51, 8034−8041

then dried under vacuum. Compound purity was confirmed through CV (see Results section and Supporting Information). Yield = 0.942 g, 43%. CHN Analysis for $[(C_{50}H_{60}N_{10}O_{10}Cu_5Gd)Cl_3(NaCl)_8(H_2O)_6]$, found (calc'd): C = 28.37 (28.35), H = 3.43 (3.53), N = 6.81 (6.61). ESI-MS (methanol) gave m/z = 727.4^{2+} (727.0^{2+} calc'd for $[GdCu_5(hpheHA_5(OH)]^{2+}$), 735.0^{2+} (736.0^{2+} calc'd for $[GdCu_5(hpheHA)_5Cl]^{2+}$).

Gd(III)[15-MC$_{Cu(II),\ N,\ S\text{-}pgHA}$-5]Cl$_3$. This compound was prepared following the procedure for **1**-hpheHA-Cl, substituting S-phenylglycineHA for S-homopheHA. Yield =1.14 g, 62.4%. CHN Analysis for $[(C_{40}H_{40}N_{10}O_{10}Cu_5Gd)Cl_3(NaCl)_{5.5}(H_2O)_{9.5}]$, found (calc'd): C = 25.38 (25.38), H = 3.17 (3.14), N = 7.41 (7.39). ESI-MS (methanol) gave m/z = 656.9^{2+} (655.9^{2+} calc'd for $[GdCu_5(pgHA)_5(OH)]^{2+}$), 664.9^{2+} (665.9^{2+} calc'd for $[GdCu_5(pgHA)_5Cl]^{2+}$), 1366.7^{+} (1365.8^{+} calc'd for $[GdCu_5(pgHA)_5Cl_2]^{+}$).

Gd(III)[15-MC$_{Cu(II),N,picHA}$-5](NO$_3$)$_{1.5}$(OH)$_{1.5}$. PicHA (500 mg, 3.62 mmol), $Cu(NO_3)_2$ (842 mg, 3.62 mmol), and $Gd(NO_3)_3$ (326.8 mg, 0.724 mmol) were stirred in a 500 mL flask with 25 mL of dimethylformamide and 8.5 mL of water. One M aqueous sodium hydroxide (7.24 mmol) was added, and the homogeneous brown solution stirred for 1 h. A 450 mL portion of acetone was then added to precipitate the MC. The flask was then stoppered and cooled in a −20 °C freezer. The precipitate was isolated by filtration on a fine glass fritted funnel, rinsed with 30 mL of cold acetone, and dried under vacuum. The purity was confirmed with CV. Yield = 929 mg, 93.4%. CHN Analysis for $[(C_{30}H_{24}N_{10}O_{10}Cu_5Gd)(NO_3)_{1.5}(OH)_{1.5}(H_2O)_{5.5}]$, found (calc'd): C = 26.20 (26.24), H = 2.48 (2.39), N = 11.93 (11.73). ESI-MS (1:1 water/methanol (v/v)) gave m/z = 585.3^{2+} (585.9^{2+} calc'd for $[GdCu_5(picHA)_5(OH)]^{2+}$), 608.3^{2+} (608.3^{2+} calc'd for $[GdCu_5(picHA)_5(NO_3)]^{2+}$), 1278.5^{+} (1277.7^{+} calc'd for $[GdCu_5(picHA)_5(NO_3)_2]^{+}$).

Cyclic Voltammetry. CV measurements were performed with a BASi Epsilon potentiostat. The counter electrode was a platinum wire, and the working electrode was a 0.0707 cm^2 glassy carbon disk that was polished with 0.05 μm alumina on velvet, rinsed, and sonicated in distilled deionized water prior to each scan. The electrochemical cell was water jacketed and held at a constant temperature of 25.0 ± 0.1 °C with a VWR 1145 refrigerated constant temperature controller. *It should be noted that strict temperature control (less than 1 °C variation) is required for accurate competition titration experiments.* The cell was protected from light with a blackout cloth to prevent **2** decomposition.[51] No evidence for decomposition was observed through the course of the experiments. CVs were taken with a scan rate of 50 mV/s. Measurements were performed at a $^{s}_{s}$pH of 8.5 in 8 mL of a 0.1 M sodium triflate solution containing 60% acetonitrile (ACN), 40% 0.1 M aqueous EPPS aqueous buffer solution. The pH was measured with a glass electrode calibrated in aqueous solutions and corrected using the reported constant.[52,53] At this pH the carboxylic acids are deprotonated and EPPS is an effective buffer.[54] No significant changes in the pH were observed through the course of the experiments. An Ag/Ag$^+$ pseudoreference electrode was employed that was composed of a silver wire in a solution of 0.01 M silver triflate and 0.1 M sodium triflate in 60% ACN, 40% water (v/v). The reference electrode was connected to the cell via a liquid junction containing 0.1 M sodium triflate in 60% ACN, 40% water solution (v/v). The reference electrode assembly was wrapped in aluminum foil to protect it from light. The silver wire was polished on fine sandpaper prior to use. The buffer, liquid junction, and silver triflate electrode solutions were prepared fresh daily. The electrode was stored in 0.1 M sodium triflate in 60% ACN, 40% water solution (v/v) between uses. All potentials are referenced to the ferrocene/ferrocenium $E_{1/2}$ measured with this electrode.

For the titrations, the concentration of **2** was 0.5 mM. Prior to the experiments, the solution was purged with nitrogen, and the cell was blanketed with nitrogen through the course of the titrations. Titrants were added as a carefully weighed solid up to the end point of the titration or the solubility limit of the MC or guest. For the titration of the MC to **2**, up to 20 equiv of MC were added. The shift in the observed $E_{1/2}$ with the change in MC concentration was fit in Origin using eq 1 below and eq 2 to solve for the concentration of free MC in solution, $[MC]_f$, where $E_c^{0'}$ and $E_f^{0'}$ are the formal potentials of the free and complexed **2**, respectively, R is the gas constant, T is the temperature, F is Faradays constant, K_{red} and K_{ox} are the association constants between the MC and the reduced and oxidized **2**, respectively, and $[\mathbf{2}]_0$ and $[MC]_0$ are the total concentrations of **2** and MC in the solution, respectively.

$$E_c^{0'} = E_f^{0'} + \frac{RT}{F}\ln\left(\frac{1 + K_{red}[MC]_f}{1 + K_{ox}[MC]_f}\right) \quad (1)$$

$$[MC]_f = \frac{-a + \sqrt{b}}{2K_{red}} \quad (2)$$

$$a = 1 + K_{red}[FcC^-]_0 - K_{red}[MC]_0$$

$$b = (1 + K_{red}[FcC^-]_0 - K_{red}[MC]_0)^2 + 4K_{red}[MC]_0$$

For the competition titrations, the MC concentration was ∼2.3 mM and up to 50 equiv of guest per **2** were titrated. The shift in the observed $E_{1/2}$ with the change in guest concentration was fit in Origin using eq 3 to solve for $[MC]_0$ and using K_{red} and K_{ox} determined from the MC binding titrations, where K_{DG} is the dissociation constant between the competitive guest and the MC, K_{Dred} is the dissociation constant between the reduced **2** and **1**, and $[G]_0$ is the total concentration of the competitive guest in solution.

$$[MC]_f = \frac{a}{3} + \frac{2}{3}\sqrt{(a^2 - 3b)}\cdot \cos\left(\frac{1}{3}\arccos\left(\frac{-2a^3 + 9ab - 27c}{2\sqrt{(a^2 - 3b)^3}}\right)\right) \quad (3)$$

$$a = K_{Dred} + K_{DG} + [FcC^-]_0 + [G]_0 - [MC]_0$$

$$b = K_{DG}([FcC^-]_0 - [MC]_0) + K_{Dred}([G]_0 - [MC]_0) + K_{Dred}K_{DG}$$

$$c = K_{Dred}K_{DG}[MC]_0$$

All titrations were performed at least three times, and the error is reported as the standard deviation.

RESULTS

The effect of the side chain on the topology of the hydrophobic cavity is best depicted by examining crystal structures of **1**. Figure 2 highlights the hydrophobic faces of **1**-picHA,[34] **1**-pgHA,[48] **1**-pheHA,[41] and **1**-hpheHA[48] using images generated from previously reported crystal structures with all bound anions and solvents removed. The structure **1**-picHA (Figure 2a) displays the planar MC face with no hydrophobic cavity.

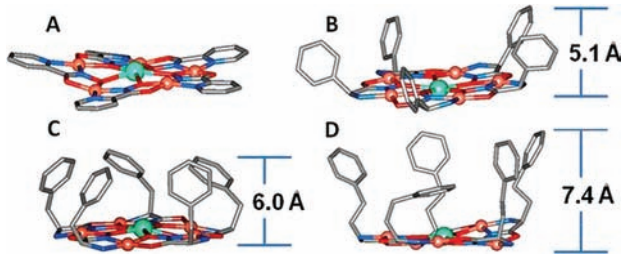

Figure 2. Structural representations of (A) **1**-picHA, (B) **1**-pgHA, (C) **1**-pheHA, and (D) **1**-hpheHA taken from previously reported crystal structures. The structures were Gd^{3+}[15-MC$_{Cu(II),\ picHA}$-5](NO$_3$),[34] Gd^{3+}[15-MC$_{Cu(II),\ pgHA}$-5](terephthalate),[48] Gd^{3+}[15-MC$_{Cu(II),\ pheHA}$-5](terephthalate),[41] and Gd^{3+}[15-MC$_{Cu(II),\ hpheHA}$-5]-(bithiophenedicarboxylate),[48] respectively.

dx.doi.org/10.1021/ic300110g | Inorg. Chem. 2012, 51, 8034−8041

Examination of **1**-pgHA, **1**-pheHA, and **1**-hpheHA reveals the phenyl side chains generate a hydrophobic cavity. The side chains of **1**-pgHA are short, rigid, and extend toward the periphery of the MC face, generating a cavity with a modest ~5.1 Å depth. The pheHA side chains are slightly longer (cavity depth is ~6.0 Å). Of note, the methylene carbon can orient the pheHA side chain toward the center of the MC face and the central Gd^{3+} ion where guests bind preferentially. With a depth of ~7.4 Å, **1**-hpheHA exhibits the largest hydrophobic cavity of the MCs presented here. The larger cavity should contribute to greater guest affinity through more extensive associative hydrophobic contacts.

Figure 3 shows previously reported crystal structures of **1**-pheHA and **1**-hpheHA with 1,4-benzene dicarboxylate guests

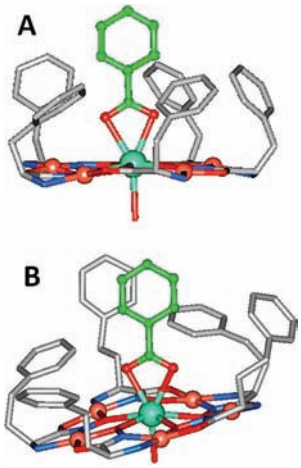

Figure 3. Structural representations of the recognition of **4** by (A) **1**-pheHA and (B) **1**-hpheHA. These images were generated from previously reported crystal structures of Gd^{3+}[15-$MC_{Cu(II),\ pheHA}$-5](1,4-benzene dicarboxylate)[41] and Gd^{3+}[15-$MC_{Cu(II),\ hpheHA}$-5](1,4-benzene dicarboxylate)[48] by removing the additional carboxylate, MCs, anions, and solvents. The pheHA side chain generates a cavity that is much shorter than **4**, while the length of the hpheHA side chain approaches that of **4**.

encapsulated in dimeric hydrophobic compartments. One carboxylate and the second MC were cropped from the figures to model the structure of **4** and highlight how the guest would be recognized by the different side chains. When coordinated bidentate to Gd^{3+}, the phenyl ring on **4** would extend ~8.0 Å from the MC face. The ~6.0 Å **1**-pheHA cavity is too short to completely encapsulate **4**, while the longer hpheHA side chain provides a better fit. Extensive π-stacking interactions with the guest are observed with both side chains. The images in Figures 2 and 3 are from crystal structures, therefore the orientation of the side chains are strongly influenced by interactions with proximal MCs in the lattice. It should be noted that the hydrophobic cavities could adopt conformations that differ from these structures in the liquid state. Given the strength of hydrophobic interactions in aqueous solutions however, it is likely that the side chains preferentially associate into hydrophobic cavities.

All MCs used in this work were synthesized by the self-assembly of one molar equivalent of Gd^{3+}, 5 equiv of Cu^{2+}, 5 equiv of ligand, and 10 equiv of base to deprotonate the ligand. **1**-pheHA was isolated as a pure solid through crystallization. **1**-pgHA, **1**-hpheHA, and **1**-picHA could not be crystallized, so they were isolated as crude powders. Inevitably, these solids contained trace Cu^{2+}-hydroxamate impurities that could not be observed with ESI-MS, CHN analysis, or UV−visible absorption spectroscopy. The presence of these impurities was evident in the CVs of **1**. Pure samples of **1** show no anodic current from 0 to 250 mV vs Fc/Fc^{+}, while the impurities display an irreversible oxidation peak with an onset at ~100 mV. For **1**-pgHA and **1**-hpheHA, these impurities were separated by flushing the complex through a shortpad of basic alumina. Pure **1**-picHA was purified by precipitation from a dimethylformamide−water solution with acetone.

Thermodynamic measurements assessing the effect of the Gd^{3+}[15-$MC_{Cu(II)}$-5] side chain on guest binding affinity were performed with CV using **2** as a redox probe. The observed potential ($E_{1/2}$) of **2** undergoes a positive shift in the presence of **1**, a result of the host stabilizing the reduced state of the guest (Figure 4). Previously established methodology[49] was

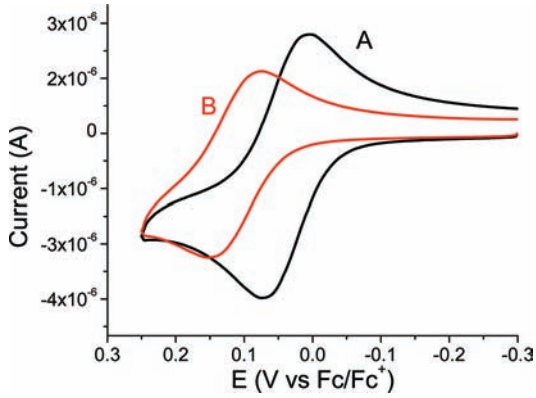

Figure 4. CVs from a MC binding titration showing **2** in the presence of 0 equiv (A) and 10 equiv (B) of **1**-hpheHA in pH 8.5 0.1 M sodium triflate solution containing 60% ACN, 40% 0.1 M aqueous EPPS buffer.

used to determine the binding affinity of **2** to **1**-pheHA based on this shift in the $E_{1/2}$. The potential shift is related to the binding affinity of the reduced **2** and oxidized ferrocenium carboxylate (**3**) by the Nernst equation (eq 1). To monitor the binding of redox inactive guests, our recently reported electrochemical competitive binding assay was utilized. In this assay, a competitive guest displaces **2** from **1**, shifting the $E_{1/2}$ back to the value of the free guest (Figure 6). The binding strength of the competitive guest is calculated based on this potential shift using the binding strength of **2** and **3**.

Previous CV titrations with **1**-pheHA were performed in 50% aqueous methanol conditions. Because of the different solubilities of **1**-pgHA and **1**-hpheHA, different solution conditions were required. Measurements presented in this work were performed at a ^{s}pH of 8.5 in a 0.1 M sodium triflate solution containing 60% acetonitrile, 40% 100 mM aqueous EPPS (v/v). These conditions were chosen to ensure that **2** is fully deprotonated[52] and displays a fully reversible redox wave throughout the titrations, as indicated by the ΔE_p and the ratio of the anodic and cathodic peak currents. The MC and guests are stable and highly soluble in these conditions. The reference electrode was carefully prepared and tested to ensure a stable potential through the course of the experiments. An Ag/Ag^{+} reference electrode with a liquid junction salt bridge, both containing 0.1 M sodium triflate in 60% acetonitrile, 40% water (v/v), provided the necessary stable potential. Control experiments demonstrate that the $E_{1/2}$ of free **2** is not affected

dx.doi.org/10.1021/ic300110g | Inorg. Chem. 2012, 51, 8034−8041

by the presence of the competitive guest in the absence of an MC, sodium chloride, or by changes in the ionic strength. Furthermore, the addition of excess sodium chloride or sodium triflate do not perturb the observed $E_{1/2}$ in the presence of the MC, suggesting that the presence of these electrolytes do not interfere with guest binding. These controls demonstrate that observed changes in $E_{1/2}$ result entirely from binding interactions of **2** and the competitive guests with **1**.

Titrations of **1** to **2** were fit using a 1:1 binding model where the guest is presumed to bind bidentate to the Gd^{3+} central metal in the hydrophobic cavity. The 1:1 binding model is justified based on previous thermodynamic investigations and the quality of the calculated fits. Previously, thermodynamic measurements of benzoate and acetate to Eu^{3+}[15-$MC_{Cu(II),pheHA}$-5](NO_3) performed with absorption spectroscopy, fluorimetry, and diffusion NMR could not detect the binding of a second guest.[46] ITC calculated that a second benzoate was bound weakly to **1**-pheHA (K_2 = 29 ± 7 M^{-1}).[44] Also, MC binding titrations are performed with an excess of the host. Thus, if a second guest is binding, it is likely binding quite weakly and it will not significantly perturb the CV data. For these reasons, the 1:1 binding model is appropriate for these measurements. Plots of $E_{1/2}$ versus the MC concentration were fit to obtain association constants between **1** and **2** (Figure 5).

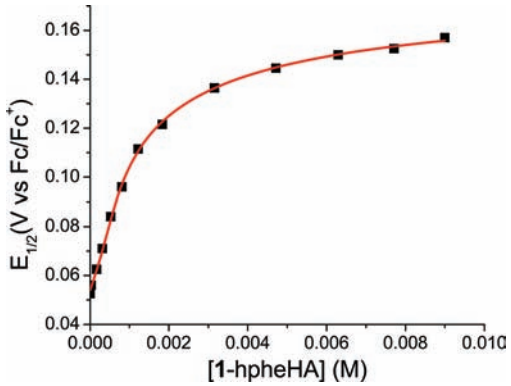

Figure 5. Plot of $E_{1/2}$ vs [**1**-hpheHA] from a MC binding CV titration in pH 8.5 0.1 M sodium triflate solution containing 60% ACN, 40% 0.1 M aqueous EPPS buffer.

Association constants between the **1** and **2** determined from the MC binding CV titrations are listed in Table 1. 1-pheHA shows a K_a of 4400 ± 700 M^{-1} with **2**. This is much larger than the previously reported value of 1040 ± 100 M^{-1} determined in 50% aqueous methanol.[45] This disparity is attributed to acetonitrile being more polar than methanol, which would lead to greater hydrophobic interactions between **2** and the hydrophobic cavity on **1**-pheHA. Also, acetonitrile is not a hydrogen bond donor and is a poor ligand; therefore, the carboxylate group on the guest and the metal ions on the MC are poorly solvated in the aqueous acetonitrile solution compared to the aqueous methanol conditions.

The binding constants of **2** with **1**-pgHA, **1**-pheHA, and **1**-hpheHA indicate that changes to the hydrophobic cavity lead to different guest recognition. **1**-pgHA and **1**-pheHA have the same affinity for **2** within error. However, **1**-hpheHA shows a much greater affinity for **2** (K_a = 12100 ± 700 M^{-1}), corresponding to a 0.5 kcal/mol enhancement with the longer side chain. *t* test analysis confirms a statistically significant difference between **1**-pheHA and **1**-hpheHA. These MC

Table 1. Thermodynamic Data for the Binding of 2, 3, and 4 to 1 in pH 8.5 0.1 M Sodium Triflate Solution Containing 60% ACN, 40% 0.1 M Aqueous EPPS Buffer

guest	ligand	K_a (M^{-1})	ΔG (kcal/mol)	p-value
ferrocene carboxylate (**2**)	picHA (NO_3)	1900 ± 100	4.47 ± 0.02	0.017[a]
	pgHA	4800 ± 400	5.02 ± 0.05	0.444[b]
	pheHA (NO_3)	4800 ± 700	5.01 ± 0.08	
	pheHA	4400 ± 700	4.97 ± 0.09	
	hpheHA	12100 ± 700	5.57 ± 0.03	0.000[b]
ferrocenium carboxylate (**3**)	picHA (NO_3)	35 ± 3	2.10 ± 0.05	0.009[a]
	pgHA	89 ± 4	2.66 ± 0.03	0.000[b]
	pheHA (NO_3)	90 ± 30	2.66 ± 0.18	
	pheHA	210 ± 30	3.18 ± 0.08	
	hpheHA	130 ± 40	2.89 ± 0.19	0.035[b]
benzoate (**4**)	pgHA	800 ± 100	3.96 ± 0.08	0.006[b]
	pheHA	1300 ± 200	4.26 ± 0.09	
	hpheHA	3000 ± 300	4.74 ± 0.06	0.000[b]

[a]P-value of two-sided *t* test corresponding to the null hypothesis that the binding constant of **1**-picHA(NO_3) is equal to the binding constant of **1**-pheHA(NO_3). [b]P-value of two-sided *t* test corresponding to the null hypothesis that the binding constant is equal to the binding constant with **1**-pheHA.

binding titrations also provide data on the affinity of **3**. For all hosts, the binding of **3** is much less than the reduced analogue, **2**, which is reasonable given that the guest is a neutral zwitterion. Weak binding affinities for zwitterions have been previously observed with **3** and phenylalanine.[44,45]

Quantitative data was sought on the separate contributions of the cavity and metal ions to guest recognition. It was hoped that comparison of the guest affinity of **1** with and without a cavity would provide this information. While the ideal comparison in this case would be to **1** with glycine hydroxamic acid or alanine hydroxamic acid ligands, the limited solubility of these MCs in the CV solution prevented the study of these complexes. To overcome solubility limitations, **1**-picHA(NO_3) was examined. Though picHA is notably different than the α-amino hydroximate ligands from the standpoints of electronics and supramolecular topology, the comparison could still be informative. As nitrate salts were necessary for **1**-picHA solubility, the binding of **2** to **1**-pheHA(NO_3) was performed to assess potential counterion effects. The binding of **1**-pheHA with Cl^- and NO_3^- counterions is the same within error, suggesting that counterion effects are minimal. **1**-picHA(NO_3) shows a relatively modest binding affinity to **2**, with a K_a value of 1900 ± 100 M^{-1}. This is significantly lower than the K_a value between **2** and **1**-pheHA(NO_3), 4800 ± 700 M^{-1}.

To expand on the observations with guest **2** and to assess how the side-chain influences enantioselectivity, competitive guest binding titrations[45] were performed to monitor the binding of redox inactive guests. Titration of the redox inactive guest to a mixture of **1** and **2** displaces the redox probe, resulting in a negative shift in $E_{1/2}$ back to the value for the free **2** (Figures 6, 7). The binding of **4**, the prototypical hydrophobic carboxylate, was examined with this competitive binding assay. The binding constants largely parallel those observed with **2**, suggesting larger cavities lead to greater binding affinities. **1**-pgHA and **1**-pheHA show K_a values of 800 ± 100 and 1300 ± 200 M^{-1}, respectively, a statistically

dx.doi.org/10.1021/ic300110g | Inorg. Chem. 2012, 51, 8034−8041

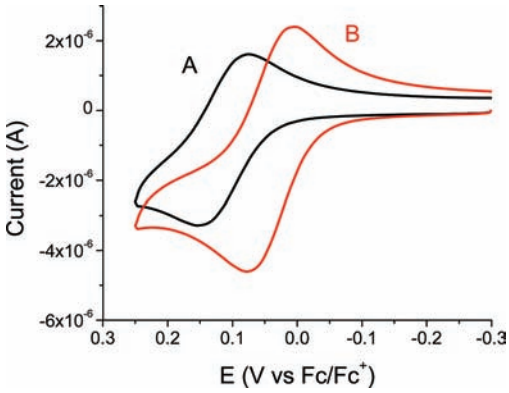

Figure 6. CVs from a competitive binding titration showing **2** in the presence of 4.7 equiv of **1**-hpheHA and 0 equiv (A) and 200 equiv (B) of S-**5** in pH 8.5, 0.1 M sodium triflate solution containing 60% ACN, 40% 0.1 M aqueous EPPS buffer.

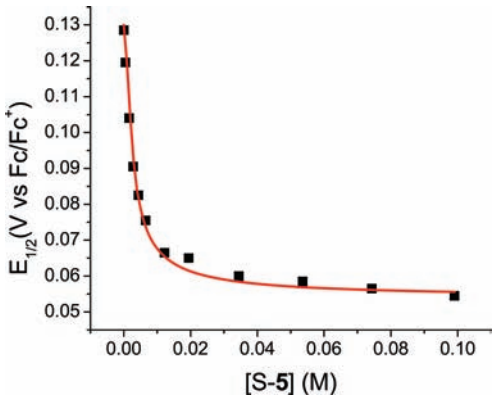

Figure 7. Plot of $E_{1/2}$ vs [S-**5**] from a competitive binding CV titration of S-**5** in pH 8.5, 0.1 M sodium triflate solution containing 60% ACN, 40% 0.1 M aqueous EPPS buffer.

significant difference. The binding affinity between **1**-hpheHA and **4** is again much larger than the other MCs, with a K_a value of 3000 ± 300 M^{-1}. Competition titrations with **1**-picHA-(NO_3) could not be modeled using the curve fitting routines available to the CV competition assay and therefore are not reported.

The previous demonstration of preferential binding of the S-**5** to **1**-pheHA (K_S/K_R = 1.22 ± 0.06) in 50% aqueous methanol[43] prompted the investigation of enantioselective binding to MCs with different side chains. The association constants of both S-**5** and R-**5** with each MC are listed in Table 2. A statistically significant preference for the S-**5** is observed with **1**-pgHA and **1**-hpheHA (K_S/K_R = 2.2 ± 0.6 and 1.5 ± 0.2 respectively). This enantioselectivity is greater than the modest K_S/K_R observed in a previous study.[43] Enantioselectivity was not observed with **1**-pheHA in these conditions.

Table 2. Thermodynamic Data on the Binding of S-5 and R-5 to 1 in pH 8.5 0.1 M Sodium Triflate Solution Containing 60% ACN, 40% 0.1 M Aqueous EPPS Buffer

guest	ligand	K_a (M^{-1})	ΔG (kcal/mol)
S-mandelate (S-**5**)	pgHA	5700 ± 1000	5.12 ± 0.11
	pheHA	2800 ± 500	4.70 ± 0.10
	hpheHA	5100 ± 500	5.05 ± 0.06
R-mandelate (R-**5**)	pgHA	2600 ± 600	4.66 ± 0.14
	pheHA	3000 ± 400	4.74 ± 0.08
	hpheHA	3400 ± 300	4.82 ± 0.04

DISCUSSION

The unique metal-rich topology and chiral cavity on Ln^{3+}[15-$MC_{Cu(II)}$-5] complexes make these types of metallocavitands promising molecules for use in catalysis or separation applications. Carboxylate guests bind reversibly to Ln^{3+}[15-$MC_{Cu(II)}$-5] metallocavitands through both electrostatic coordination of the carboxylate to metal ions on the MC face and hydrophobic interactions between the guest and the hydrophobic cavity. One important and previously unexplored facet of Ln^{3+}[15-$MC_{Cu(II)}$-5] guest recognition is the role of the side-chain in guest affinity. Side-chain variation has the potential to provide a facile route to preparing highly selective hosts given the general synthesis Ln^{3+}[15-MC-5] complexes through self-assembly. Solid-state studies suggest that the ligand side chains play a significant role in guest recognition. The length and flexibility of the phenyl side-chain influence the cavity size and the extent that the host can converge on a bound guest.[48] This report on the thermodynamics of carboxylate binding to **1** with picHA, S-pgHA, S-pheHA, and S-hpheHA side-chains provides the first quantitative demonstration of enhanced guest affinity and enantioselectivity through Ln^{3+}[15-$MC_{Cu(II)}$-5] side chain variation.

This study utilizes the guest binding model that has been established based on trends in guest binding affinity and extensive crystallographic characterization. Carboxylates are presumed to bind primarily to the central Gd^{3+} ion in the hydrophobic cavity of **1**, forming a 1:1 host−guest complex. 2:1 and 2:2 MC:guest complexes form with bridging guests, such as dicarboxylates or isonicotinate. However, these MC dimers are likely weakly associated and are not expected to form with the nonbridging guests studied herein. Considering the possibility of forming 1:2 host−guest complexes, while two guests are often observed crystallographically, the binding of a second guest is frequently not detected experimentally or is very weak (<30 M^{-1} for **1**-pheHA).[44] The least-squares fitting routines used in this work operate under the assumption that only one guest is bound. This is justified by the aforementioned observations and the nature of the CV binding constant measurements. The MC binding titrations are performed with an excess of host; thus, the very weak binding of a second guest would have little impact on potential shifts. For the competitive binding assay, an excess of the host is again utilized relative to the redox probe **2**. Also, the assay examines the displacement of **2** from **1**. Since the probe molecule cannot report on sequential binding when it is displaced, the competitive binding assay only detects 1:1 binding.

MC binding titrations were performed to measure the binding strength of **2** and **3**. **2** binds equally to **1**-pheHA and **1**-pgHA, though a significant binding strength enhancement is observed with **1**-hpheHA. This difference is attributed to greater hydrophobic interactions with the larger hpheHA hydrophobic cavity. An estimate for cavity size can be obtained from crystal structures of **1** that were previously reported (Figure 2).[48] These structures show the S-pgHA side-chain generates a hydrophobic cavity with a depth of ∼5.1 Å. **1**-pheHA has a ∼ 6.0 Å cavity, while **1**-hpheHA has a ∼ 7.4 Å cavity. Crystal structures of **2** and ferrocene dicarboxylate bound to Ln^{3+}[15-MC-5] complexes suggest that the most distant hydrogen atom on **2** would extend about 7.6 Å from the

dx.doi.org/10.1021/ic300110g | Inorg. Chem. 2012, 51, 8034−8041

Gd^{3+} ion.[45] Thus, the larger **1**-hpheHA cavity is better suited for encapsulating **2**.

To understand the separate electrostatic and hydrophobic contributions to guest recognition better, attempts were made to measure guest binding to **1** with no cavity. Unfortunately, limited host solubility prevented the study of the most appropriate MCs without cavities, **1** prepared with glycine hydroxamic acid and alanine hydroxamic acid, necessitating analysis of the picHA complexes. The relatively small binding constant between **1**-picHA and **2** reflects the absence of the hydrophobic cavity. Unfortunately, the electronic and structural differences between picHA and the α-aminoHA ligands prevents the direct relation of differences in binding constants to effects of the cavity. The picHA pyridyl group is about 4 log units less basic than the amine on α-aminoHA ligands. Thus, the **1**-picHA Gd^{3+} ion is expected to be more Lewis acidic and have stronger electronic interactions with carboxylate guests. Also, the large pyridyl group on picHA would have a slightly greater hydrophobic interaction with guests than the two carbon chain on the α-aminoHA ligand backbone. Thus the ~0.5 kcal/mol binding enhancement seen with **1**-pheHA over **1**-picHA is expected to be an underestimation of the contribution of the hydrophobic cavity.

Looking at the competition titration data with **4**, all MCs show a weaker affinity than for **2**. As the pK_a's of the two guests are effectively the same,[55,56] the greater affinity for **2** is attributed to more extensive associative interactions and a greater hydrophobic effect with the larger guest. **1**-hpheHA again shows significantly greater affinity than **1**-pheHA and **1**-pgHA. Structural representations of **4** bound to **1**-pheHA and **1**-hpheHA suggest that this selectivity is a result of the larger hpheHA cavity size. **4** would extend beyond the ~6.0 Å hydrophobic cavity on **1**-pheHA, while the **1**-hpheHA cavity provides a better fit. Notably, **1**-pheHA shows significantly greater affinity for **4** than **1**-pgHA. Such a difference was not observed with **2**. This discrepancy likely arises from the relative flexibility of the ligand side chains and the shape of the guests. The pgHA side chain is a rigid phenyl ring that is oriented toward the periphery of the MC face. The pheHA side chain contains a flexible methylene carbon, allowing the phenyl ring to rotate toward the center of the MC (Figures 2b, 2c). Crystal structures of **1**-pheHA complexes show that the flexibility of the pheHA side chain allows for extensive π-stacking and hydrophobic interactions with **4** or other guests bound bidentate to the central metal in the center of the cavity (Figure 3A). While this is advantageous, the flexibility also introduces a reorganization energy penalty to guest inclusion. The rigid **1**-pgHA does not incur as significant a reorganization energy penalty; however, it will have minimal interactions with a carboxylate bound at its center. Thus for **4**, **1**-pheHA likely displays stronger binding because the flexibility of the side-chain allows for more extensive interactions with the guest. The taller **1**-pheHA cavity also contributes. With **2**, the ferrocene moiety extends toward the periphery of the MC face where it can likely interact with the pgHA side-chains. This effect of guest shape and the smaller reorganization energy involved with **1**-pgHA likely cause the lack of discrimination seen with **2**.

In addition to the enhanced guest binding affinity, variation of the MC side chains can improve enantioselectivity. Both **1**-pgHA and **1**-hpheHA preferentially bind the S-enantiomer of **5**. **1**-pheHA does not display this enantioselectivity. Though a trend is not evident that relates enantioselectivity to chain length or flexibility, these results clearly demonstrate that variation of the side chain provides a route to enhanced enantioselectivity. Impressively, the enantioselectivity observed with **1**-pgHA is much greater than the modest 1.22 K_S/K_R value between **1**-pheHA and **5** in 50% aqueous methanol.[43] It is likely that the rigidity of the pgHA side chain contributes to the greater enantioselectivity. The chiral anion selectivity seen with **1**-pgHA is not record breaking, as selectivities of 9 or greater have been observed with steroidal receptors[57,58] and select other systems.[59,60] However, the selectivity is on par with or exceeds the anion enantioselectivity displayed by certain β-cyclodextrins.[10] The selectivity is promising for these first-generation ligands, especially considering the dearth of metallamacrocycles that display enantioselective guest binding[8,61] and the general difficulty of enantioselective *anion* binding.

The lack of chiral discrimination displayed by **1**-pheHA for **5** is surprising given the modest enantioselectivity observed in 50% aqueous methanol.[43] This difference likely arises from the acetonitrile conditions utilized in this experiment leading to a different binding mode than in the aqueous methanol conditions. Previous measurements in aqueous methanol showed that the enantiomers of **5** display significantly stronger affinity for **1**-pheHA than **2** and **4**, which was attributed to the guest being bound via a 5-membered chelate ring through the hydroxyl group and a carboxylate oxygen atom. The binding strengths of **2**, **4**, and **5** are more similar in the 60% aqueous acetonitrile conditions, which could be indicative of the guests adopting the same bidentate carboxylate binding mode. A different binding mode for **5** in aqueous methanol and acetonitrile could cause the different enantioselectivity (Table 3). Unfortunately, crystal structures of **5** bound to **1** could not be obtained from any solvent. The precise origin of the chiral discrimination in **1** will be explored in future work.

Table 3. K_S/K_R Values for 5 Binding to 1 in pH 8.5 0.1 M Sodium Triflate Solution Containing 60% ACN, 40% 0.1 M Aqueous EPPS Buffer

host	K_S/K_R	p-value
1-pgHA	2.2 ± 0.6	0.004[a]
1-pheHA	0.9 ± 0.2	0.588[a]
1-hpheHA	1.5 ± 0.2	0.001[a]

[a]P-value of two-sided *t* test corresponding to the null hypothesis that the binding constant of the S-enantiomer is equal to the binding constant of the R-enantiomer.

CONCLUSION

The findings presented here quantitatively demonstrate how peripheral organic substituents in the secondary coordination sphere can influence molecular recognition at a metal center in metallocavitands. These results also provide the first evidence that altering the Ln^{3+}[15-MC-5] side chain can lead to enhanced guest binding affinity and enantioselectivity. In particular, the significant enantioselectivity found with **1**-pgHA provides reason for further study of chiral recognition or catalysis with Ln^{3+}[15-MC-5] hosts. Highly elaborate side chains could be designed to perform useful chiral separations or catalysis. Ln^{3+}[15-MC-5] complexes are a general platform derived from α-amino hydroxamic acids, which can be synthesized from α-amino acids in short syntheses. Given the facile self-assembly of Ln^{3+}[15-MC-5] complexes and the potentially vast ligand libraries that can be derived from the

dx.doi.org/10.1021/ic300110g | Inorg. Chem. 2012, 51, 8034−8041

plethora of commercially available, relatively inexpensive chiral α-amino acids, one can envision high throughput screening methodology could be utilized to rapidly detect highly selective Ln^{3+}[15-MC-5] metallocavitands suitable for chiral guest resolution or catalysis.

■ ASSOCIATED CONTENT

Supporting Information

Further details are given in Figure S1 and Table S1. This material is available free of charge via the Internet at http://pubs.acs.org.

■ AUTHOR INFORMATION

Corresponding Author

*E-mail: vlpec@umich.edu.

Notes

The authors declare no competing financial interest.

■ REFERENCES

(1) Hof, F.; Craig, S. L.; Nuckolls, C.; Rebek, J. J. *Angew. Chem., Int. Ed.* **2002**, *41*, 1488.
(2) Whittell, G. R.; Hager, M. D.; Schubert, U. S.; Manners, I. *Nat. Mater.* **2011**, 10.
(3) Tiefenbacher, K.; Dube, H.; Ajami, D.; Rebek, J., Jr. *Chem. Commun.* **2011**, *47*, 7341.
(4) Hui, J. K. H.; MacLachlan, M. J. *Coord. Chem. Rev.* **2010**, *254*, 2363.
(5) MacGillivray, L. R.; Atwood, J. L. *J. Solid State Chem.* **2000**, *152*, 199.
(6) Yoshizawa, M.; Klosterman, J. K.; Fujita, M. *Angew. Chem., Int. Ed.* **2009**, *48*, 3418.
(7) Pluth, M. D.; Bergman, R. G.; Raymond, K. N. *Acc. Chem. Res.* **2009**, *41*, 1650.
(8) Fiedler, D.; Leung, D. H.; Bergman, R. G.; Raymond, K. N. *J. Am. Chem. Soc.* **2004**, *126*, 3674.
(9) Hambury, G. A.; Borovkov, V. V.; Inoue, Y. *Chem. Rev.* **2008**, *108*, 1.
(10) Easton, C. J.; Lincoln, S. F. *Chem. Soc. Rev.* **1996**, 163.
(11) Atwood, J. L.; Koutsantonis, G. A.; Raston, C. L. *Nature* **1994**, *368*, 229.
(12) Liu, S.; Gan, H.; Hermann, A. T.; Rick, S. W.; Gibb, B. C. *Nat. Chem.* **2010**, *2*, 847.
(13) Jiang, X.-B.; Leeuwen, P. W. N. M. v.; Reek, J. N. H. *Chem. Commun.* **2007**, 2287.
(14) Kersting, B.; Lehmann, U. *Adv. Inorg. Chem.* **2009**, *61*, 407.
(15) Schmidtchen, F. P. *Chem. Soc. Rev.* **2010**, *39*, 3916.
(16) Fabbrizzi, L.; Foti, F.; Taglietti, A. *Org. Lett.* **2005**, *7*, 2603.
(17) Allevi, M.; Bonizzoni, M.; Fabbrizzi, L. *Chem.—Eur. J.* **2007**, *13*, 3787.
(18) O'Neil, E. J.; Smith, B. D. *Coord. Chem. Rev.* **2006**, *250*, 3068.
(19) Damsyik, A.; Lincoln, S. F.; Wainwright, K. P. *Inorg. Chem.* **2006**, *45*, 9834.
(20) Frischmann, P. D.; Gallant, A. J.; Chong, J. H.; MacLachlan, M. J. *Inorg. Chem.* **2008**, *47*, 101.
(21) Fabbrizzi, L.; Licchelli, M.; Perotti, A.; Rabaioli, G.; Sacchi, D.; Taglietti, A. *J. Chem. Soc., Perkin Trans. 2* **2001**, 2108.
(22) Fabbrizzi, L.; Licchelli, M.; Taglietti, A. *Dalton Trans.* **2003**, 3471.
(23) Steinfield, G.; Lozan, V.; Kersting, B. *Angew. Chem., Int. Ed.* **2003**, *42*, 2261.
(24) Käss, S.; Gregor, T.; Kersting, B. *Angew. Chem., Int. Ed.* **2005**, *45*, 101.
(25) Richeter, S.; J. Rebek, J. *J. Am. Chem. Soc.* **2004**, *126*, 16280.
(26) Zelder, F. H.; Rebek, J., Jr. *Chem. Commun.* **2006**, 753.
(27) Mezei, G.; Zaleski, C. M.; Pecoraro, V. L. *Chem. Rev.* **2007**, *107*, 4933.
(28) Gibney, B. R.; Wang, H.; Kampf, J. W.; Pecoraro, V. L. *Inorg. Chem.* **1996**, *35*, 6184.
(29) Lah, M. S.; Gibney, B. R.; Tierney, D. L.; Penner-Hahn, J. E.; Pecoraro, V. L. *J. Am. Chem. Soc.* **1993**, *115*, 5857.
(30) Kessissoglou, D. P.; Kampf, J. W.; Pecoraro, V. L. *Polyhedron* **1994**, *13*, 1379.
(31) Stemmler, A. J.; Kampf, J. W.; Pecoraro, V. L. *Angew. Chem., Int. Ed. Engl.* **1996**, *35*, 2841.
(32) Szumna, A. *Chem. Soc. Rev.* **2010**, *39*, 4274.
(33) Stemmler, A. J.; Barwinski, A.; Baldwin, M. J.; Young, V.; Pecoraro, V. L. *J. Am. Chem. Soc.* **1996**, *118*, 11962.
(34) Stemmler, A. J.; Kampf, J. W.; Kirk, M. L.; Atasi, B. H.; Pecoraro, V. L. *Inorg. Chem.* **1999**, *38*, 2807.
(35) Dallavalle, F.; Remelli, M.; Sansone, F.; Bacco, D.; Tegoni, M. *Inorg. Chem.* **2010**, *49*, 1761.
(36) Tegoni, M.; Remelli, M. *Coord. Chem. Rev.* **2012**, *256*, 289.
(37) Zaleski, C. M.; Depperman, E. C.; Kampf, J. W.; Kirk, M. L.; Pecoraro, V. L. *Inorg. Chem.* **2006**, *45*, 10022.
(38) Lim, C. S.; Jankolovits, J.; Kampf, J. W.; Pecoraro, V. L. *Chem.—Asian. J.* **2010**, *5*, 46.
(39) Mezei, G.; Kampf, J. W.; Pan, S.; Poeppelmeier, K. R.; Watkins, B.; Pecoraro, V. L. *Chem. Commun.* **2007**, 1148.
(40) Cutland, A. D.; Halfen, J. A.; Kampf, J. W.; Pecoraro, V. L. *J. Am. Chem. Soc.* **2001**, *123*, 6211.
(41) Lim, C.-S.; Van Noord, A. C.; Kampf, J. W.; Pecoraro, V. L. *Eur. J. Inorg. Chem.* **2007**, *2007*, 1347.
(42) Zaleski, C. M.; Lim, C. S.; Cutland-Van Noord, A. D.; Kampf, J. W.; Pecoraro, V. L. *Inorg. Chem.* **2011**, *50*, 7707.
(43) Lim, C. S.; Jankolovits, J.; Zhao, P.; Kampf, J. W.; Pecoraro, V. L. *Inorg. Chem.* **2011**, *50*, 4832.
(44) Lim, C. S.; Kampf, J. W.; Pecoraro, V. L. *Inorg. Chem.* **2009**, *48*, 5224.
(45) Jankolovits, J.; Kampf, J. W.; Maldonado, S.; Pecoraro, V. L. *Chem.—Eur. J.* **2010**, *16*, 6786.
(46) Tegoni, M.; Tropiano, M.; Marchio, L. *Dalton Trans.* **2009**, 6705.
(47) Cutland, A. D.; Malkani, R. G.; Kampf, J. W.; Pecoraro, V. L. *Angew. Chem., Int. Ed.* **2000**, *39*, 2690.
(48) Jankolovits, J.; Lim, C.-S.; Mezei, G.; Kampf, J. W.; Pecoraro, V. L. *Inorg. Chem.* **2012**, *51* (8), 4527.
(49) Mendoza, S.; Castaño, E.; Meas, Y.; Godínez, L. A.; Kaifer, A. E. *Electroanalysis* **2004**, *16*, 1469.
(50) Jankolovits, J.; Andolina, C. M.; Kampf, J. W.; Raymond, K. N.; Pecoraro, V. L. *Angew. Chem., Int. Ed.* **2011**, *50*, 9660.
(51) Ali, L. A. C., A.; Kemp, T. J. *J. Chem. Soc., Dalton Trans.* **1973**, 1468.
(52) Espinosa, S.; Bosch, E.; Roses, M. *Anal. Chem.* **2000**, *72*, 5193.
(53) Perrin, D. D.; Dempsey, B. *Buffers for pH and Metal Ion Control*; Chapman and Hall: London, U.K., 1979.
(54) Azab, H. A.; Nour, K. M. A. *J. Chem. Eng. Data* **1999**, *44*, 678.
(55) Matsue, T.; Evans, D. H.; Osa, T.; Kobayashi, N. *J. Am. Chem. Soc.* **1985**, *107*, 3411.
(56) Azab, H. A.; Ahmed, I. T.; Mahmoud, M. R. *J. Chem. Eng. Data* **1995**, *40*, 523.
(57) Lawless, L. J.; Blackburn, A. G.; Ayling, A. J.; Perez-Payan, M. N.; Davis, A. P. *J. Chem. Soc., Perkin Trans. 1* **2001**, 1329.
(58) Brotherhood, P. R.; Davis, A. P. *Chem. Soc. Rev.* **2010**, *39*, 3633.
(59) Konishi, K.; Yahara, K.; Toshishige, H.; Aida, T.; Inoue, S. *J. Am. Chem. Soc.* **1994**, *116*, 1337.
(60) Lin, W.-C.; Tseng, Y.-P.; Lin, C.-Y.; Yen, Y.-P. *Org. Biol. Chem.* **2011**, *9*, 5547.
(61) Brumaghim, J. L.; Michels, M.; Raymond, K. N. *Eur. J. Org. Chem.* **2004**, *22*, 4552.